A Microdevice for Studying Intercellular Electromechanical Transduction in Adult Cardiac Myocytes

Xu Zhang[a], **Qian Wang**[a], **Brian Gablaski**[b], **Xiaojin Zhang**[b], **Pamela Lucchesi**[b], and **Yi Zhao**[a]
Yi Zhao: zhao.178@osu.edu
[a]Laboratory for Biomedical Microsystems, Department of Biomedical Engineering, The Ohio State University, Columbus, OH, 43210 USA

[b]Center for Cardiovascular and Pulmonary Research, Nationwide Children's Hospital, Columbus, OH, 43205 USA

Abstract

Intercellular electromechanical transduction in adult cardiac myocytes plays an important role in regulating heart function. The efficiency of intercellular electromechanical transduction has so far been investigated only to a limited extent, which is largely due to the lack of appropriate tools that can quantitatively assess the contractile performance of interconnected adult cardiac myocytes. In this paper we report a microengineered device that is capable of applying electrical stimulation to the selected adult cardiac myocyte in a longitudinally connected cell doublet and quantifying the intercellular electromechanical transduction by measuring the contractile performance of stimulated and un-stimulated cells in the same doublet. The capability of applying selective electrical stimulation on only one cell in the doublet is validated by examining cell contractile performance while blocking the intercellular communication. Quantitative assessment of cell contractile performance in isolated adult cardiac myocytes is performed by measuring the cell length change. The proof-of-concept assessment of gap junction performance shows that the device is useful in studying the efficiency of gap junctions in adult cardiac myocytes that are most relevant to synchronized pumping performance of native myocardium. Collectively, this work provides a quantitative tool for studying intercellular electromechanical transduction and is expected to develop a comprehensive understanding of the role of intercellular communications in various heart diseases.

Introduction

Heart diseases are the leading causes of mortality in the United States, and account for nearly 24% of all deaths.[1] Although drug therapy and cardiac assistive devices have gained rapid development in the past few decades, the prognosis of heart diseases remains poor.[2] A prominent portion of the heart dysfunction stems from the disorder of heart muscles, namely myocardial diseases, which may cause heart failure and arrhythmic sudden death. In heart muscle, cardiac myocytes are the basic contractile units that determine the magnitude and

Correspondence to: Yi Zhao, zhao.178@osu.edu.

frequency of myocardial contractile function. Particularly, the contractile performance of heart muscles is regulated by force generation of individual cardiac myocytes, and mechanical transmissions between the neighbouring cells and from the cells to the extracellular matrix. In the past two decades, extensive molecular and electrophysiological studies have been conducted to unravel the underlying mechanism of myocardial disorders.[3] Results of these studies, including gap junction downregulation,[4] altered gap junction distribution,[5] and reduced gap junction conductance,[6] suggest that defective intercellular communication in cardiac myocytes is an underlying cause of left ventricular dysfunction in several heart diseases. However, the efficiency of electromechanical transduction, which is the direct measure of intercellular communication within the myocardium, has so far been experimentally explored only to a limited extent. This is largely due to the lack of appropriate tools that can quantitatively assess the contractile performance of interconnected adult cardiac myocytes.

Intercellular communication within heart muscle is mainly orchestrated by a thin structure located at the longitudinal end of the cardiac myocytes, named the intercalated disc. The intercalated discs connect individual cardiac myocytes into an electrochemical syncytium and are primarily responsible for electromechanical transmission during heart contraction.[7] Until recently, the properties of the intercalated discs have been primarily studied within the intact animal heart or using perfused tissue blocks.[8–11] However, the intrinsic heterogeneity and complexity of the native cardiac environment, which contains multiple types of interconnected cells that are morphologically and functionally distinct, have hindered the quantitative study of cardiac cells communication. In this perspective, an *ex vivo* cell-based model using adult cardiac myocytes is preferred, because it is immune to the complications arising from heterogeneity in electrical excitation and contraction in the native cardiac environment,[12, 13] while the adult cardiac myocytes isolated from the hearts largely preserve the characteristics of native myocardium.

Current studies investigating intercellular communication using cell-based models include the quantification of dye transfer using microinjection,[14] scrape loading,[15] electroporation,[16] gap FRAP (fluorescence recovery after photobleaching),[17] LAMP (local activation of molecular fluorescent probe),[18] etc.; the recording of intercellular calcium propagation;[19] and the measurement of electrical conductance using electrophysiological approaches.[20] Although these methods can provide quantitative measurements of cell-to-cell communication, their applications in adult cardiac myocytes are largely restricted by a number of intrinsic limitations.[21] The dye transfer and the calcium propagation methods provide accurate measurements on gap junction permeability, yet the functional information such as force generation and force transmission is overlooked. The electrophysiological approach using dual patch clamp is exquisitely sensitive in assaying the electrical conductance between cells. However, the technique is not conducive for high throughput assay, because patch clamping is a slow, labor-intensive and expensive technique that requires specialized equipment and experienced technicians. A recent study used microfluidic systems to examine cardiac myocyte coupling by combining cell manipulation, $[Ca^{2+}]_i$ measurement and dual patch clamp analysis on a single chip.[22] In this work, nevertheless, both cells in the cell pair were stimulated, which complicated data analyses

and interpretations in terms of electromechanical transmission. Likewise, the well commercialized field stimulators, such as Grass (Grass Technologies, Warwick, RI) and IonOptix (IonOptix LLC, Miltion, MA), apply electric fields to all the adult cardiac myocytes in the culture well. It is, therefore, difficult to separate the contractile performances due to external electrical stimulation and due to intercellular communication.

In this study, a microdevice was developed for the quantitative assessment of intercellular cardiac mechanical performance using isolated adult cardiac myocytes, which circumvented the current technical pitfalls. This device applies electrical stimulations to a selected adult cardiac myocyte in a longitudinally connected cell doublet, and quantifies the intercellular electro-mechanical transduction by measuring the contractile performance of stimulated and un-stimulated cells in the same doublet. Since the contractile performance of the un-stimulated cells due to direct electrical stimulation is eliminated, this work provides a quantitative tool for studying intercellular electro-mechanical transduction and is expected to develop a comprehensive understanding of the role of intercellular communication in various heart diseases.

Experimental

Microengineered approach for studying intercellular communication

The working principle of the microdevice is illustrated in Figure 1. A longitudinally connected cell doublet is positioned in the electrodes array where one cell resides on top of an electrode finger (myocyte B), and the other one in the same cell doublet resides between two neighboring electrodes (myocyte A). When a pulse voltage is applied to the electrodes pair, the cell sitting between the two electrodes is subjected to a local electric field and contracts accordingly, while the cell on the electrode finger is not stimulated due to the isopotential electrode surface. The contraction of the un-stimulated cell is hence solely due to the intercellular communication with the stimulated cell through the intercalated disc. During the whole process, the cell length changes over time in both the stimulated and the un-stimulated cells provide a quantitative measure of the intercellular communication.

Microchip fabrication and system implementation

The core component of the microchip is the electrode stimulator, which was fabricated by patterning an array of interdigitated microelectrodes on a dielectric glass slide (75 cm × 25 cm) using a standard photolithographic process (Figure 2a). Specifically, a layer of positive photoresist (S1813, Shipley) was first spin-coated on a pre-cleaned glass slide, and patterned under an aligner by photolithography. The glass slide with patterned photoresist structures was then deposited with a layer of 20-nm-thick titanium (Ti) followed by a layer of 100-nm-thick gold (Au) by E-beam evaporation. The Ti layer was used for improving the adhesion between the glass substrate and the Au electrode. After deposition, the photoresist layer was lifted-off by N-methyl-2-pyrrolidinone (NMP), leaving the patterned microelectrodes on the glass substrate. Given the typical length of adult cardiac myocytes used in this study of ~ 80–100 μm, the gap between the two electrodes was designed as 70 μm to ensure that the maximal voltage can be applied to the cell lying across the two neighbouring electrodes. The width of electrodes was designed as 200 μm so that the second cell in the doublet can

completely reside within the electrode surface. All pairs of electrodes were numbered to facilitate the selective electrical stimulation. Figures 2b&c show the components and the assembly of the device. The microchip was mounted on a custom-designed microscope adaptor fitting for the stage of the upright microscope. A PDMS well (15mm in diameter) was then attached to delineate the active area of the interdigitated electrodes for electrical cell stimulation. An array of spring contact probes (Interconnect Devices, Kansas City, KS) were pushed against two U-shape clips in order to contact the numbered electrode leads patterned on the microchip. Finally, a flexible flat cable (FFC) was used to connect the contact probes with a function generator (Agilent 3220A, Agilent Technologies, Santa Clara, CA) for electrical stimulation (Figure 2d).

Cell isolation and immunofluorescence staining

Hearts were removed from terminally anaesthetized Sprague-Dawley rats (source: Harlan, sex: male, age: 60–100 days). Adult cardiac myocytes were isolated from the left ventricle by sequentially perfusing with Tyrodes buffer (131 mM NaCl, 4 mM KCl, 10 mM HEPES buffer, 0.2 mM $CaCl_2$, 1 mM $MgCl_2$, 10mM 2,3-Butanedione monoxime, 10mM Glucose. 2min), perfusion buffer (113mM NaCI, 4.7mM KCl, 0.6mM KH_2PO_4, 0.6mM Na_2HPO_4, 1.2mM $MgSO_4$-$7H_2O$, 0.032mM Phenol red, 12mM $NaHCO_3$, 10mM $KHCO_3$, 10mM HEPES buffer, 30mM Taurine, 10mM 2,3-Butanedione monoxime, 5.5mM Glucose. 6min), and digestion buffer (1X perfusion burffer, 0.25mg/ml Liberase blendzyme, 0.14mg/ml Trypsin, 18μM $CaCl_2$. 10min) using a Langendorff system. After filtering (250μm filter), centrifuging (560 rpm for 2 min) and re-suspending in plating media (1X MEM, 5% Fetal bovine serum, 10mM 2,3-Butanedione monoxime, 100U/ml Penicillin, 2mM L-Glutamine), cells were switched to culture media (1X MEM, 0.1mg/ml Myocyte bovine serum albumin, 100U/ml Penicillin, 2mM L-Glutamine) and incubated for 30 min. Plated cells were then washed, gently detached and then replated in the device. This procedure yielded >95% viable cardiac myocytes, of which ~3% to 8% were longitudinally connected doublets.

To confirm the integrity of cell-cell junctions in the isolated adult cardiac myocytes doublets, immunostaining for the intercalated disc proteins Connexin 43 (Cx43) and N-cadherin were performed following the established protocols.[23] Briefly, the cardiac myocytes were fixed with 2% parafomaldehyde in PBS for 10 mins at the room temperature, and permeabilized with 1% Triton X-100 for 30 mins. After blocking with 2% goat serum for 2 hrs, cells were sequentially incubated with the primary antibodies (Anti-Connecxin-43 antibody, Sigma-Aldrich, St. Louis, MO; Anti-N-Cadherin-antibody, BD Biosciences, San Jose, CA) overnight at 4°C and then the secondary antibodies (Alexa Fluor 488 conjugated goat anti-rabbit IgG antibody and Dynabeads conjugated sheep anti-mouse IgG antibody, Life Technologies, Grand Island, NY) for 1 hr at room temperature. After immunostaining, the samples were examined using an Olympus IX51 microscope (Olympus, Melville, NY), where both gap junction (Cx43, red) and adherens junction (N-cadherin, green) were present in the intercalated disc (Figure 3), suggesting that the cell-cell connections are largely preserved during the isolation procedure.

Electrical cell stimulation

Before the examination of intercellular electro-mechanical transduction, the device was sterilized and coated with laminin (5 μg/ml) overnight at the room temperature. The cells were then transferred into the culture well on the device and cultured for a few hours to allow the cell attachment on the glass surface. Prior to the electrical stimulation, the culture media was replaced by the contractile buffer (131 mM NaCl, 4 mM KCl, 10 mM HEPES buffer, 1 mM $CaCl_2$, 1 mM $MgCl_2$, 10mM Glucose) in order to facilitate cell contraction. Afterwards, an electric voltage pulse with a frequency of 1 Hz and a width of 8 ms was applied between the two neighbouring electrode fingers of a selected electrodes pair where the subject cell doublet lay. The voltage magnitude ramped slowly from zero to an appropriate value to ensure that the selected cell was appropriately stimulated: a lower voltage was not able to induce cell contraction while a higher voltage may cause immediate cell death. To determine the threshold voltage for cell excitation, the cell length change under the applied voltage was monitored. When a threshold of the electric voltage optimal for cell stimulation was identified, the voltage magnitude was maintained as low as possible and kept constant during the whole stimulation process.

Image analysis

Changes in cell lengths upon electrical stimulation were recorded at 7 frames per second (fps) (cellSens Entry 1.5, Olympus) with a CCD camera (Olympus DP71) attached to an upright microscope (Olympus BX51). A dual gooseneck illuminator (B&B microscopes, Pittsburgh, PA) was used as a complementary light source to obtain a high brightness. The morphological parameters of the cells (cell length and cell orientation) were obtained using ImageJ (National Institutes of Health, US), where the cell contractility was derived by dividing the cell length reduction upon contraction by the original un-stimulated cell length.

Statistic analysis

Cell contractility was determined from 15–20 cells with three independent experiments, and expressed as mean ± standard deviation from 6 measurements (unless otherwise stated). The normalized cell contractility was defined using the contractility of each cell at the threshold voltage as the reference. The differences between groups were analyzed by one-way ANOVA, with $p<0.05$ set as statistically significant. Non-linear least squares regression method (MATLAB R2009b, MathWorks, Natick, MA) was used for data fitting.

Results and discussion

Finite element analysis of selective electrical stimulation

To implement selective electrical stimulation, the applied electric field had to be confined within one cell while keeping the other un-stimulated. The localized electric field was examined using finite element analysis (FEA) (Figure 4). The result showed that when a voltage bias (1 V) was applied to two neighboring electrodes (200 μm in width and 70 μm in spacing), the electric field induced in the dielectric region between the two electrodes ($\sim1.5\times10^4$ V/m) was an order of magnitude larger than that on the electrode surface ($<10^3$ V/m). The induced electric field in the neighbourhood due to the electrical coupling between

the excited electrodes and the adjacent floating electrodes ($\sim5\times10^3$ V/m) was also much lower than the threshold that can induce cell contraction ($\sim1.3\times10^4$ V/m in this study). Consequently, with appropriate voltage magnitude, the cell lays itself between the excited electrodes would contract, while the cell on the electrode surface would not be stimulated. In other words, contraction of the cell on the electrode surface, if any, should be solely due to the communication with the neighbouring cell through intercellular electro-mechanical transduction.

Characterization of cell contraction by electrical stimulation

Electrical cell stimulation by interdigitated electrodes was experimentally demonstrated by applying a local electric field to a single adult cardiac myocyte lying perpendicularly across the 70 μm-wide gap between two neighbouring electrodes (Figure 5a). This cell was stimulated at three different frequencies (0.5Hz, 1.0 Hz and 2.0 Hz). The cell length change showed that the frequency of the induced cell contraction was fairly consistent with that of the electrical stimulation (Figure 5b & c). The cell contractility varied with the stimulation frequency. Specifically, 1.0 Hz stimulation led to the greatest cell length change (Figure 5d). This frequency was selected as the stimulation frequency in the subsequent studies.

The effect of the magnitude of the applied voltage on cell contractile performance was also investigated by measuring the cell length changes in a number of single cells that lay themselves across the two excited electrodes (Figure 6a). It was found there is an optimal "window" of electrical voltage that can induce cell contraction. Given the electrode configuration and the gap distance between the neighboring electrodes, most cells were stimulated to contract under a voltage between 1.0 V and 1.3 V. A lower voltage could not induce cell contraction while a higher voltage led to immediate cell death. Within the voltage "window", there was no significant correlation between the cell contractility and the voltage magnitude (Figure 6b). This result had a fairly good agreement with the "all-or-none" law for electrical stimulation of cardiac myocytes, namely, the cell responds to the best of its ability if the stimulus is above the threshold.[24]

Since the cells across the electrode gap oriented randomly, the electric field loaded on each cell may vary with the cell orientation. This was taken into account by re-plotting the cell contractility in a polar coordinate system (Figure 6c). Here, the cell orientation was defined by the intersection angle between the major cell axis and the direction of the electric field, *i.e.* 0° denotes that the cell oriented parallel to the applied electric field while 90° refers to an orthogonal relationship. The effect of the cell orientation on the electrical field along the major cell axis was expressed by:

$$U = d \times E_e \cos\theta^{-1} + U' \quad (1)$$

where U is the applied voltage between two electrodes, U' denotes the voltage drop within the dielectric medium (culture media), E_e denotes the effective electrical field along the major cell axis, and d denotes the gap between two neighboring electrodes. Assuming that all cardiac myocytes have the same electrical and mechanical properties (*i.e.* the E_e value that can induce cell contraction is approximately the same for all the cells), the threshold voltage that applied between two electrodes was a function of $cos\theta$ (R^2=0.64, Figure 6d). As

the cell orientation ramped from 0° to 90°, the threshold voltage from 0.9 V to 1.5 V (Figure 6c). It was noted that in this study the minimal voltage capable of inducing contraction in adult cardiac myocytes was 0.9 V, corresponding to an electric field intensity of 1.3×10^4 V/m. At such an intensity level, the applied electric field was able to raise the membrane potential from the baseline of about −90 mV to the threshold of ~-75 mV for evoking an action potential followed by a cell contraction.[2] This appropriate intensity of the electric field capable of inducing contraction varies heavily with the animal species, the cell type, the waveform of the electrical stimuli, the electrode configuration and the culturing environment. For instance, previous studies reported 50V/m pulses for adult rat cardiac myocytes cultured in ACCITT medium;[25] $4–7.5 \times 10^3$ V/m pulses for neonatal rat ventricular myocytes cultured in DMEM medium;[26, 27] 5.0×10^2 V/m rectangular pulses for neonatal rat ventricular myocytes cultured on the collagen scaffold;[28] 5.5×10^2 V/m rectangular pulses for adult rabbit cardiac myocytes cultured in Base Krebs Solution;[22] and 1.4×10^3 V/m pulses for Guinea pig cardiac myocytes cultured in Krebs Henseleit buffer.[29]

Electrical stimulation of the selected adult cardiac myocyte in cell doublets

Selective electrical stimulation was validated by examining the cell contractions in a doublet while blocking the intercellular communication by adding 1.08 mM 1-Heptanol (Sigma-Aldrich) to the culture media and treating for 5 minutes. Gap junctions are known to play an important role in cardiac conduction by facilitating electrical and chemical communication between adjacent myocytes.[30] In particular, gap junctions provide low resistance pathways for intercellular ion flow and determine the level of action potential propagation within the myocardium. The dysfunction of gap junctions, therefore, causes abnormal coupling between cardiac myocytes and ultimately results in impaired cardiac conductions as well as reduced myocardium pumping performance, as found in many heart diseases.[31] Accordingly, the gap junction has been well recognized as a pharmacological target for the treatment of arrhythmia and other heart diseases[32, 33]. Heptanol is commonly used as a non-specific gap junction blocker in cardiac intercellular communication studies.[34–36] Before gap junction blockade, the cell on the electrode surface (un-stimulated) and the cell between the two excited electrodes (stimulated) both exhibited noticeable contractions (the average contractility of the un-stimulated and stimulated cells were ~ 4.5% and 8.5%, respectively), as evidenced by the cell length shortenings (Figure 7a). After the gap junction was blocked, however, the cell on the electrode surface no longer exhibited periodic length changes with the average contractility lower than 0.5%, while the cell between the two electrodes was still in contraction with the average contractility ~5% (Figure 7b), suggesting that the contraction of the un-stimulated cell was solely due to the intercellular communication with the stimulated cell through the gap junction. It was noted that the rhythmical contraction of the stimulated cell was somewhat disrupted after the gap junction blocking. This is believed due to the use of heptanol as the gap junction blocker. In addition to blocking almost all subtypes of gap junction channels in myocardium (Cx43, Cx40, Cx45), heptanol also inhibits voltage-sensitive calcium current and reduces $[Ca^{2+}]_i$.[37] Considering the pivotal roles of calcium current and $[Ca^{2+}]_i$ in the excitation-contraction coupling process in cardiac muscle, the non-junctional effects caused by heptanol may account for the disturbed contractile profile of the stimulated cell.

Finally, a proof-of-concept study was conducted to examine the performance of the device in assessing the gap junction performance within adult cardiac myocytes doublets (Figure 8). The first cell doublet was isolated following the regular protocol as mentioned in the experimental section (18 μM $CaCl_2$ in the digestion buffer), while the second cell doublet was prepared with the reduced calcium concentration in the digestion buffer (14.5 μM $CaCl_2$). In the first cell doublet (Figure 8a & b), the two cells contracted at the same frequency and at the same phase, which were in register with the applied electrical stimulation. The contractility of the stimulated cell was slightly greater than that of the un-stimulated one. The result suggested that the gap junction in the first pair was well-preserved and was able to synchronize the contractile functions in the coupled cell. This is similar to that in a healthy heart where all cells are contracting synchronously so that the ventricle can exhibit a maximal pumping performance. In the second cell doublet (Figure 8c & d), the un-stimulated cell exhibited an irregular contractile performance with a discernible phase shift comparing to the stimulated cell. The unsynchronized contractions indicated an impaired conductance in the gap junction or an altered electro-mechanical coupling mechanism, which may represent the conditions of myocardium in the cardiac fibrillation.

During the cell isolation procedure, the extracellular calcium level is most critical to the constituent of the final collection.[38, 39] This is because calcium ions are necessary to stabilize the intercellular connections in ventricular cardiac myocytes by maintaining the integrity of plasma membranes surrounding the gap junctional plaques.[40] A low calcium concentration reduces the proportion of intact cell doublets, while a high calcium concentration results in a significant decrease in the yield of viable cells. The trade-off between the number of cell doublets and the overall cell viability has restricted the applicable calcium concentrations into a narrow window to collect the end-to-end connected cell doublets. A concentration of 14.5 μM is close to the lower limit of calcium concentration (~ 14 μM according to a previous report[41]) required for the survival of junctional connections during an isolation process. Although cells still connected to their neighbors in this circumstance (Figure 8c), the intercellular connection was weak and the gap junctional communication was impaired as demonstrated by the asynchronous contractile performance of the second cell doublet (Figure 8d).

Besides the capability of examining gap junction change due to varying calcium concentration, the reported device is also able to examine alterations in the gap junction performance due to other extrinsic and intrinsic factors that may cause asynchronous contraction and the contractility degradation between the two cells in a longitudinally connected doublet. High throughput assay is possible when the reported device is coupled with microfluidic channels. In this perspective, this work not only develops a quantitative platform for studying the role of intercellular electro-mechanical transduction under various heart diseases, but also provides a powerful tool to assess the possibilities of pharmacological approaches towards efficient clinical therapies.

Conclusions

This paper describes a microengineered device that is capable of applying electrical stimulation to the selected adult cardiac myocytes in a longitudinally connected cell doublet

and keeping the other cell un-stimulated. The capability of applying selective electrical stimulation on only one cell in the doublet was validated by examining cell contractile performance while blocking the intercellular communication. Quantitative assessment of cell contractile performance in isolated adult cardiac myocytes was performed by measuring the cell length change. The proof-of-concept assessment of gap junction performance showed that the device is useful in studying the efficiency of gap junctions in adult cardiac myocytes that are most relevant to synchronized pumping performance of native myocardium. The device also provides an *ex vivo* model with direct contractile performance measurement for enhancing the understanding of the role of intercellular electro-mechanical transduction under various controlled conditions in contractile cells.

Acknowledgments

References

1. Hoyert DL, Xu J. Natl Vital Stat Rep. 2012; 61:65.

2. Klabunde, RE. Cardiovascular Physiology Concepts. Philadelphia: Lippincott Williams & Wilkins; 2011.

3. Severs NJ, Coppen SR, Dupont E, Yeh HI, Ko YS, Matsushita T. Cardiovasc Res. 2004; 62:368–377. [PubMed: 15094356]

4. Kaprielian RR, Gunning M, Dupont E, Sheppard MN, Rothery SM, Underwood R, Pennell DJ, Fox K, Pepper J, Poole-Wilson PA, Severs NJ. Circulation. 1998; 97:651–660. [PubMed: 9495300]

5. Sepp R, Severs NJ, Gourdie RG. Heart. 1996; 76:412–417. [PubMed: 8944586]

6. Akar FG, Nass RD, Hahn S, Cingolani E, Shah M, Hesketh GG, DiSilvestre D, Tunin RS, Kass DA, Tomaselli GF. Am J Physiol Heart Circ Physiol. 2007; 293:H1223–H1230. [PubMed: 17434978]

7. Akester AR. J Anat. 1981; 133:161–179. [PubMed: 7333947]

8. Aistrup GL, Kelly JE, Kapur S, Kowalczyk M, Sysman-Wolpin I, Kadish AH, Wasserstrom JA. Circ Res. 2006; 99:e65–e73. [PubMed: 16960102]

9. Lamont C, Luther PW, Balke CW, Wier WG. J Physiol. 1998; 512(Pt 3):669–676. [PubMed: 9769412]

10. Cooklin M, Wallis WR, Sheridan DJ, Fry CH. Circ Res. 1997; 80:765–771. [PubMed: 9168778]

11. Peters NS, Green CR, Poole-Wilson PA, Severs NJ. Circulation. 1993; 88:864–875. [PubMed: 8394786]

12. Komuro I, Katoh Y, Kaida T, Shibazaki Y, Kurabayashi M, Hoh E, Takaku F, Yazaki Y. J Biol Chem. 1991; 266:1265–1268. [PubMed: 1702436]

13. Balligand JL, Kelly RA, Marsden PA, Smith TW, Michel T. Proc Natl Acad Sci U S A. 1993; 90:347–351. [PubMed: 7678347]

14. Frank DK, Szymkowiak B, Josifovska-Chopra O, Nakashima T, Kinnally KW. Head Neck-J Sci Spec. 2005; 27:794–800.

15. Sai K, Kanno J, Hasegawa R, Trosko JE, Inoue T. Carcinogenesis. 2000; 21:1671–1676. [PubMed: 10964098]

16. Anagnostopoulou A, Cao J, Vultur A, Firth K, Raptis L. Mol Oncol. 2007; 1:226–231. [PubMed: 19383296]

17. Abbaci M, Barberi-Heyob M, Stines JR, Blondel W, Dumas D, Guillemin F, Didelon J. Biotechnol J. 2007; 2:50–61. [PubMed: 17225250]

18. Dakin K, Zhao Y, Li WH. Nat Methods. 2005; 2:55–62. [PubMed: 15782161]

19. Charles AC, Merrill JE, Dirksen ER, Sanderson MJ. Neuron. 1991; 6:983–992. [PubMed: 1675864]

20. Durig J, Rosenthal C, Halfmeyer K, Wiemann M, Novotny J, Bingmann D, Duhrsen U, Schirrmacher K. Brit J Haematol. 2000; 111:416–425. [PubMed: 11122080]

21. Abbaci M, Barberi-Heyob M, Blondel W, Guillemin F, Didelon J. Biotechniques. 2008; 45:33–52. 56–62. [PubMed: 18611167]

22. Klauke N, Smith G, Cooper JM. Lab Chip. 2007; 7:731–739. [PubMed: 17538715]

23. Luke RA, Beyer EC, Hoyt RH, Saffitz JE. Circ Res. 1989; 65:1450–1457. [PubMed: 2478314]

24. Bowditch HP. Ber Sachs Ges Wiss. 1871; 23:652–689.

25. Berger HJ, Prasad SK, Davidoff AJ, Pimental D, Ellingsen O, Marsh JD, Smith TW, Kelly RA. Am J Physiol. 1994; 266:H341–H349. [PubMed: 8304516]

26. Xia Y, Buja LM, Scarpulla RC, McMillin JB. Proc Natl Acad Sci U S A. 1997; 94:11399–11404. [PubMed: 9326621]

27. McDonough PM, Glembotski CC. J Biol Chem. 1992; 267:11665–11668. [PubMed: 1376309]

28. Radisic M, Park H, Shing H, Consi T, Schoen FJ, Langer R, Freed LE, Vunjak-Novakovic G. Proc Natl Acad Sci U S A. 2004; 101:18129–18134. [PubMed: 15604141]

29. Brady AJ, Warren JB, Poole-Wilson PA, Williams TJ, Harding SE. Am J Physiol. 1993; 265:H176–H182. [PubMed: 8342632]

30. Jongsma HJ, Wilders R. Circ Res. 2000; 86:1193–1197. [PubMed: 10864907]

31. Rohr S. Cardiovasc Res. 2004; 62:309–322. [PubMed: 15094351]

32. Salameh A, Dhein S. Biochim Biophys Acta. 2005; 1719:36–58. [PubMed: 16216217]

33. Eloff BC, Gilat E, Wan X, Rosenbaum DS. Circulation. 2003; 108:3157–3163. [PubMed: 14656916]

34. Qi X, Varma P, Newman D, Dorian P. Circulation. 2001; 104:1544–1549. [PubMed: 11571250]

35. Takens-Kwak BR, Jongsma HJ, Rook MB, Van Ginneken AC. Am J Physiol. 1992; 262:C1531–C1538. [PubMed: 1616013]

36. Kimura H, Oyamada Y, Ohshika H, Mori M, Oyamada M. Exp Cell Res. 1995; 220:348–356. [PubMed: 7556443]

37. Matchkov VV, Rahman A, Peng H, Nilsson H, Aalkjaer C. Br J Pharmacol. 2004; 142:961–972. [PubMed: 15210581]

38. Powell T, Terrar DA, Twist VW. J Physiol. 1980; 302:131–153. [PubMed: 6251204]

39. Hohl CM, Altschuld RA, Brierley GP. Arch Biochem Biophys. 1983; 221:197–205. [PubMed: 6830255]

40. Muir AR. J Anat. 1967; 101:239–261. [PubMed: 6040076]

41. Wittenberg BA, White RL, Ginzberg RD, Spray DC. Circ Res. 1986; 59:143–150. [PubMed: 2427246]
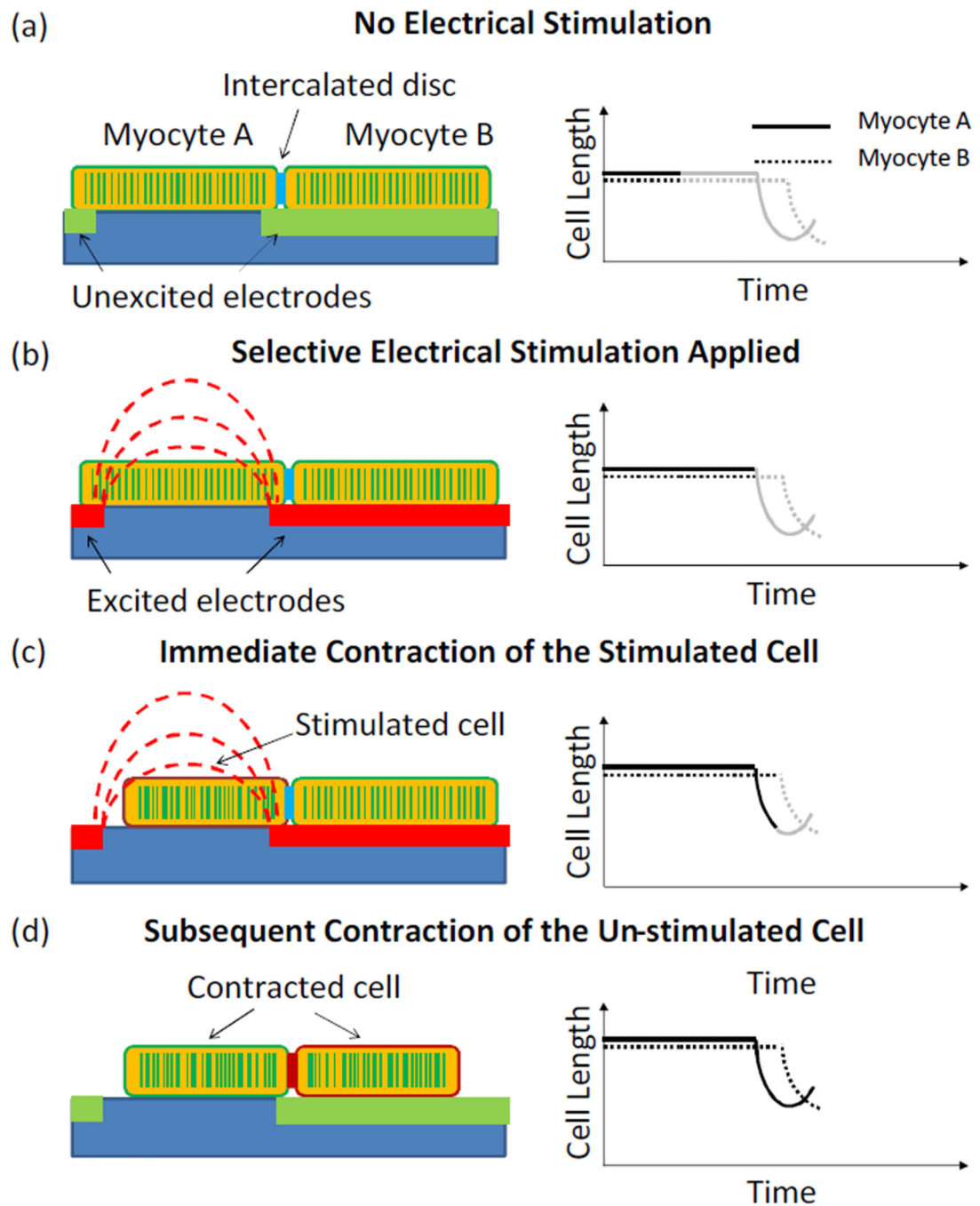
Fig. 1.
Schematics of the microengineered approach for intercellular communication studies. (a) A cardiac myocytes doublet was positioned in the electrodes array with one cell lying between two neighboring electrodes and the other one lying on top of an electrode finger. (b) Electrodes were selectively excited, giving rise to a localized electric field. (c) Myocyte A contracted upon the electrical stimulation. (d) Myocyte B contracted due to the electromechanical coupling with myocyte A through the intercalated disc. Left: Schematics

of electrode stimulation and cell contraction; Right: Schematic curves showing the changes in cell length.
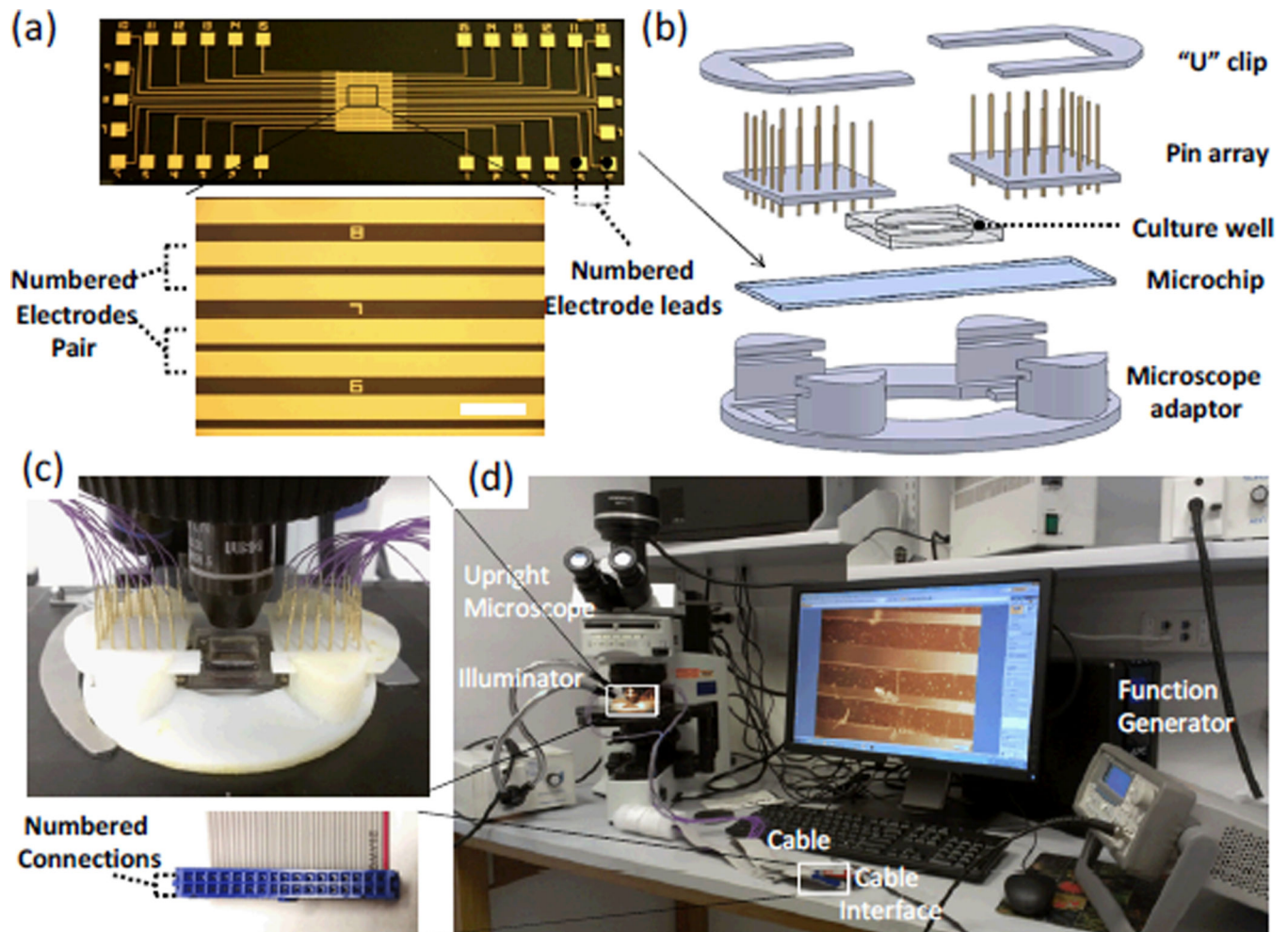
Fig. 2.
Experimental setup for selective electrical stimulation and cell contraction assessment: (a) Micropatterned interdigigated electrode array on a glass slide. Scale Bar=500μm. (b) Schematic showing the components of the selective stimulation device, including two U-shape clips, spring contact probes arrays, a cell culture well, an on-chip electrode stimulator and a microscope adaptor. (c) The assembled selective stimulation device was mounted on the stage of an upright microscope. (d) The experimental setup used for applying selective electrical stimulation and measuring cell contractile performance. The inset shows the cable interface with the numbered connections.
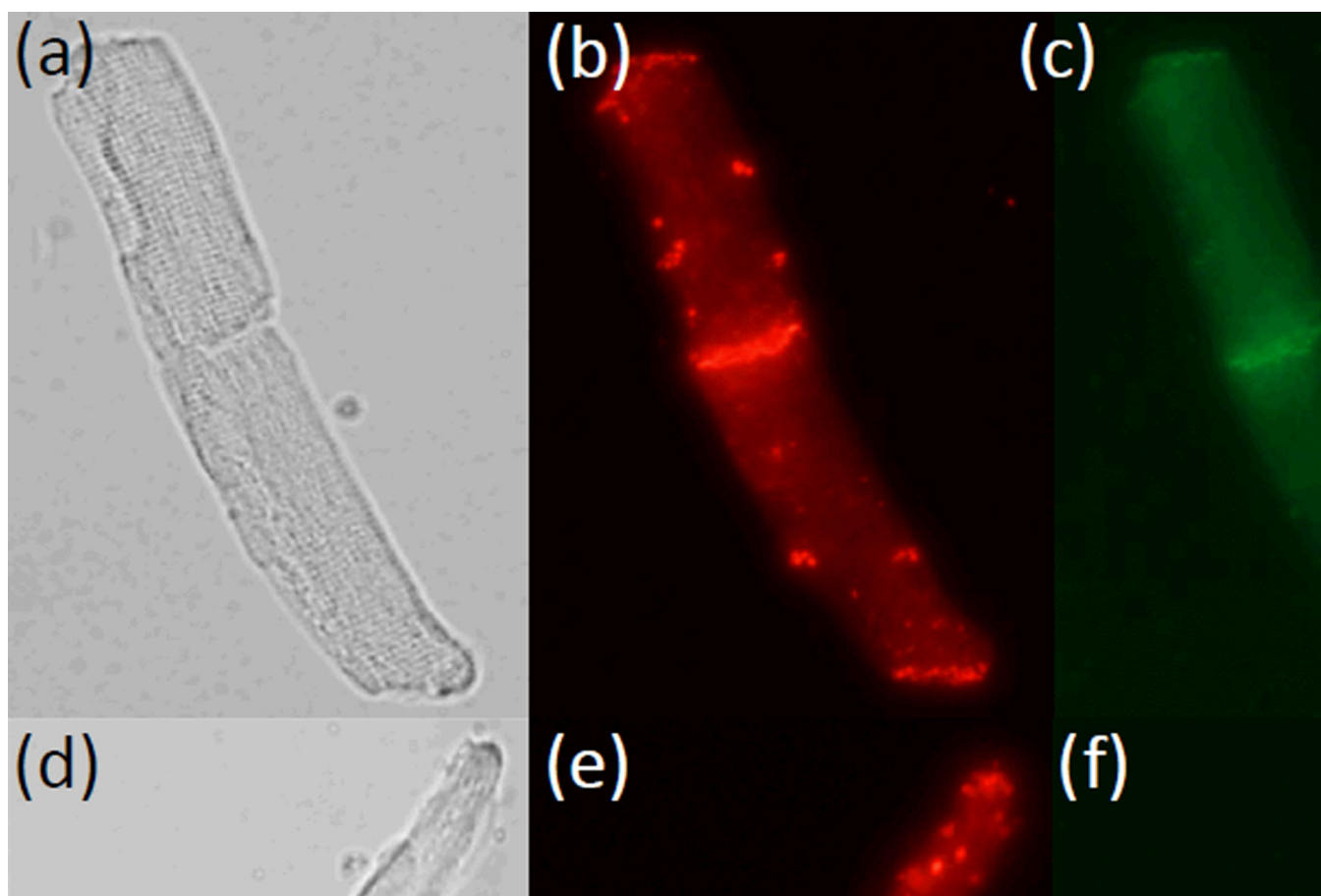
Fig. 3.
Immunofluorescence staining of the intercalated discs in isolated doublets of adult cardiac myocytes. (a,d) Bright field images of myocytes doublets. (b,e) Immunostaining of Connexin 43. (c, f) Immunostaining of N-cadherin. Both Connexin 43 and N-cadherin in the intercalated discs were well-preserved.
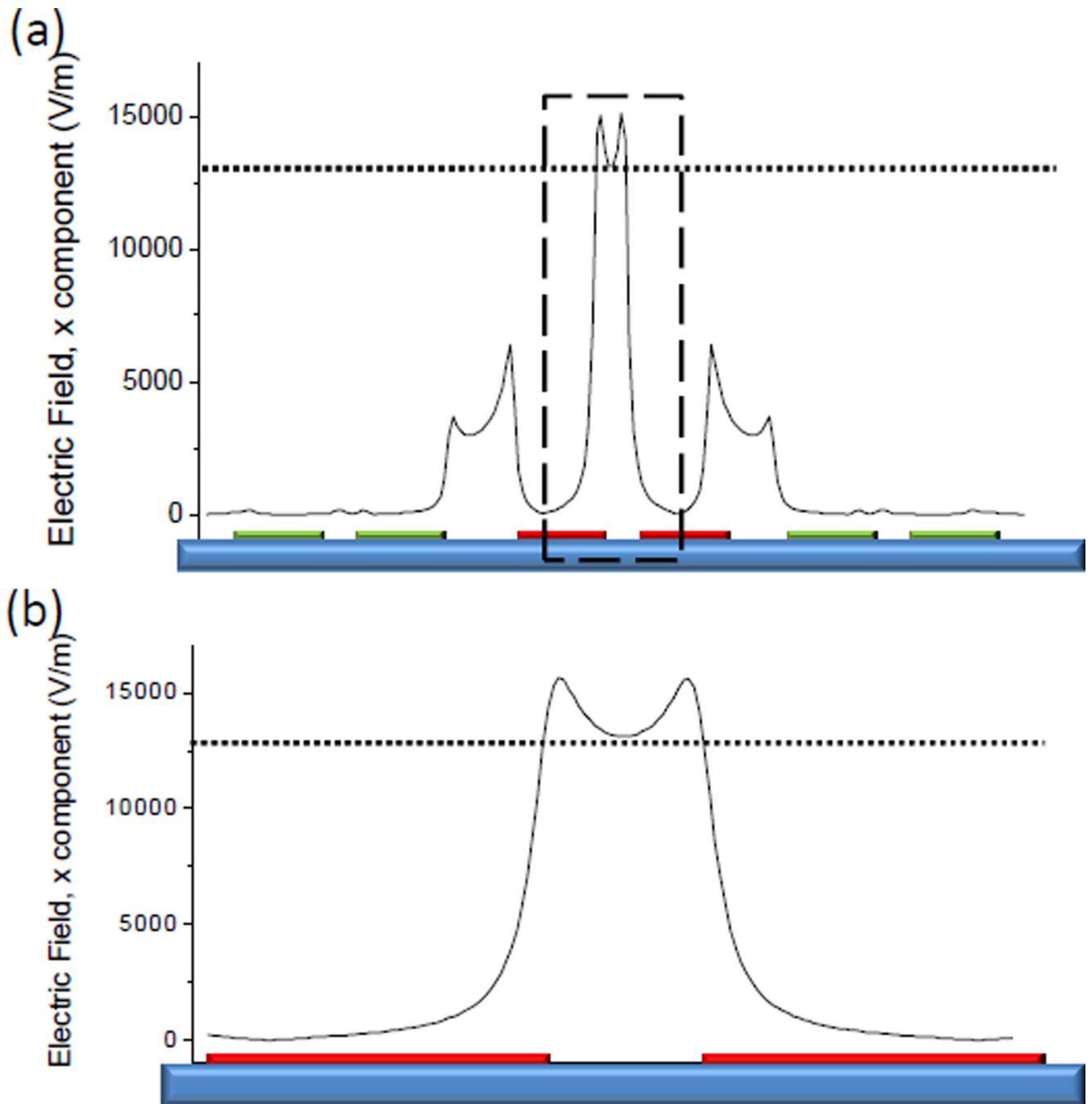
Fig. 4.
Finite element analysis of the localized electric field. (a) The electric field in the close vicinity of the excited electrodes (red). Since the cells lie parallel to the substrate, only the absolute value of the lateral component of the electric field was plotted. (b) Close-in view of the dashed rectangle in (a). The electric field induced in the dielectric region between the two electrodes is much greater than that on the electrode surface. The dotted line denotes the approximate electric field threshold for inducing cell contraction.
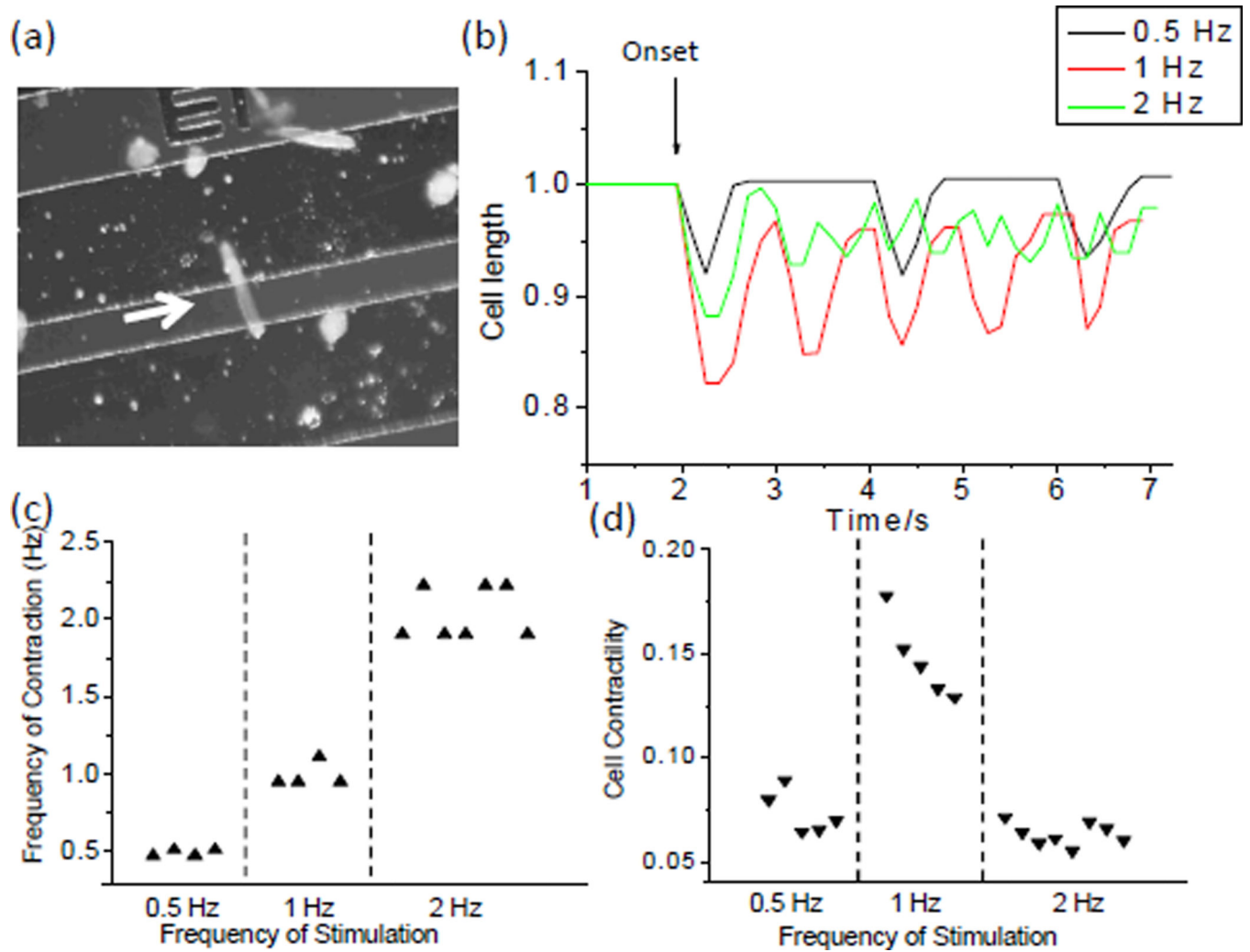
Fig. 5.
Electrical stimulation of single adult cardiac myocytes. (a) Micrograph showing a cardiac myocyte lying across the gap between the neighboring electrodes. (b) Contractile performance of the cell responding to electrical stimuli at different frequencies. (c) Comparison of the frequency of cell contraction and the frequency of electrical stimulation. (d) Relation between the cell contractility and the frequency of electrical stimulation.
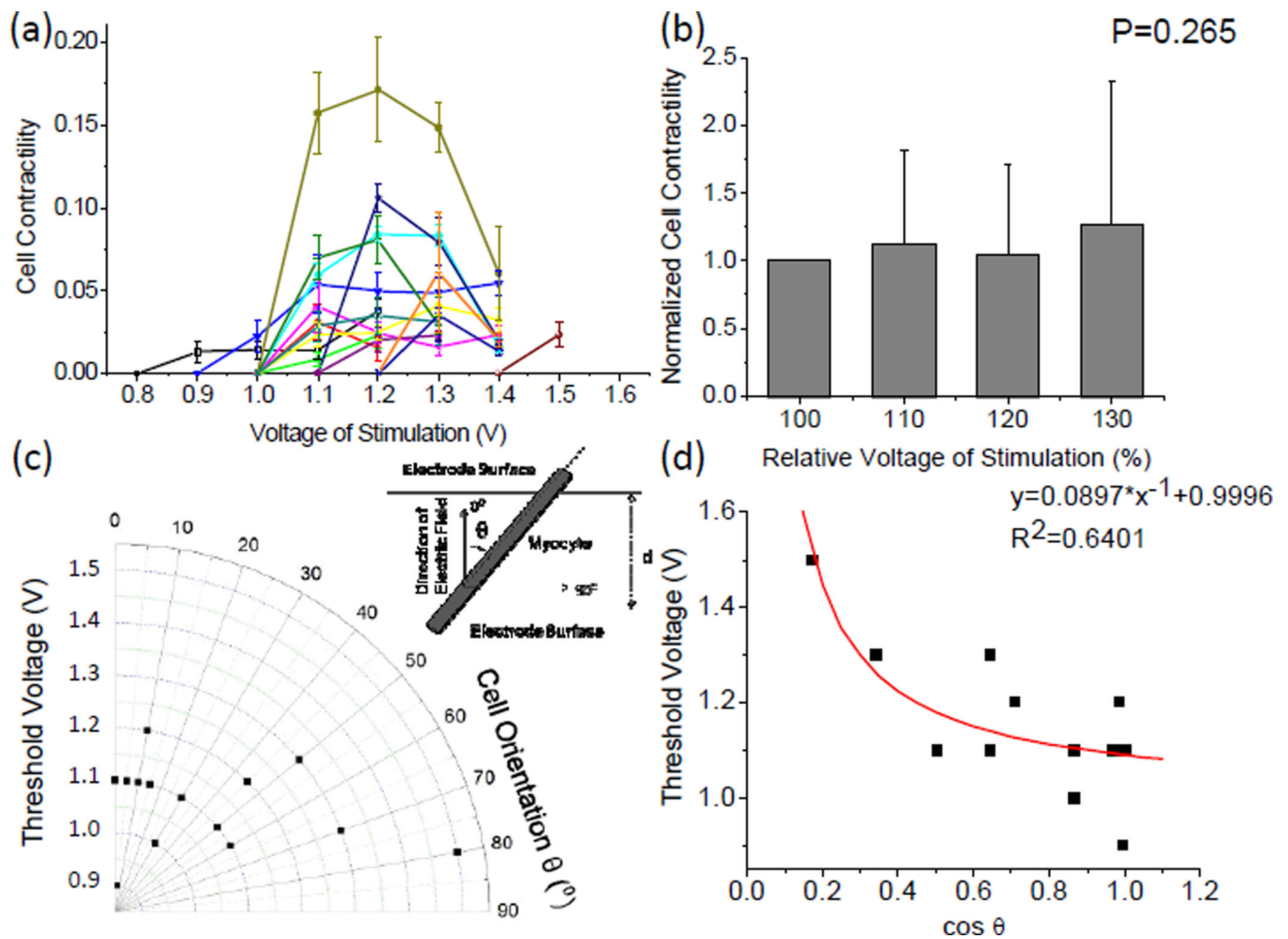
Fig. 6.
Characterization of cell contractility upon electrical stimulation. (a) Cell contractility as a function of the applied voltage. Each curve represents the data recorded from one cell. (b) Statistics showing the effect of applied voltage on the cell contractility. The stimulation voltage is presented as a relative value using the threshold voltage of each cell as the reference (100%). The normalized cell contractility is defined using the contractility of each cell at the threshold voltage as the reference. (c) Threshold voltage for inducing cell contraction as a function of cell orientation. Inset: definition of cell orientation (θ). (d) Threshold Voltage as a function of the cosine value of cell orientation with a nonlinear fitting curve.
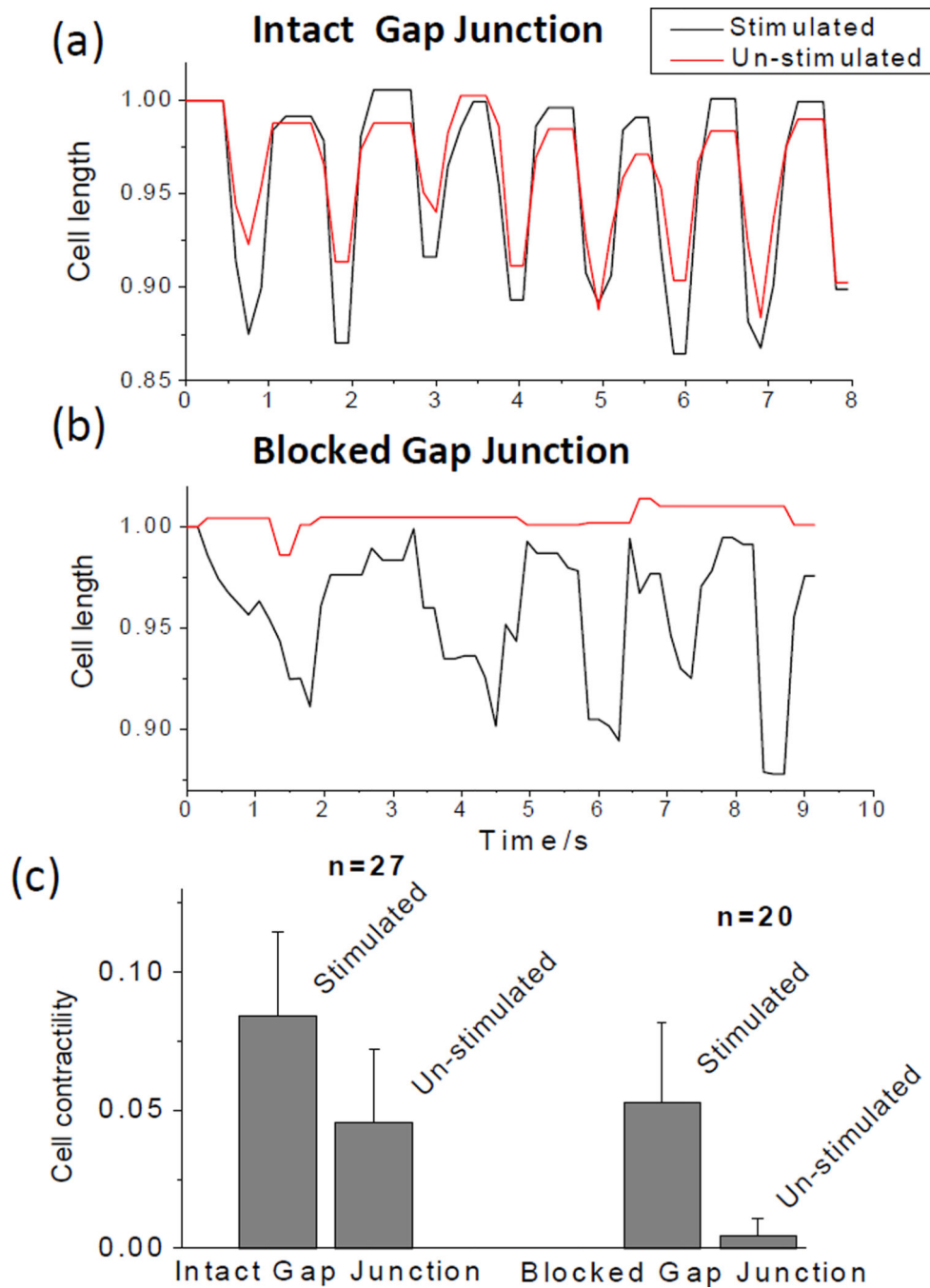
Fig. 7.
Contractile performances of two cells in a longitudinally connected cell-cell doublet (a) before and (b) after a gap junction blocker was applied. (c) Statistics showing the effect of the gap junction blocker on cell contractility. Cell contractility was determined from three independent experiments, and expressed as mean ± standard deviation. Both cells exhibited discernible contraction before the blockage of gap junction, while the un-stimulated cell no longer exhibited periodical length change after the gap junction was blocked.
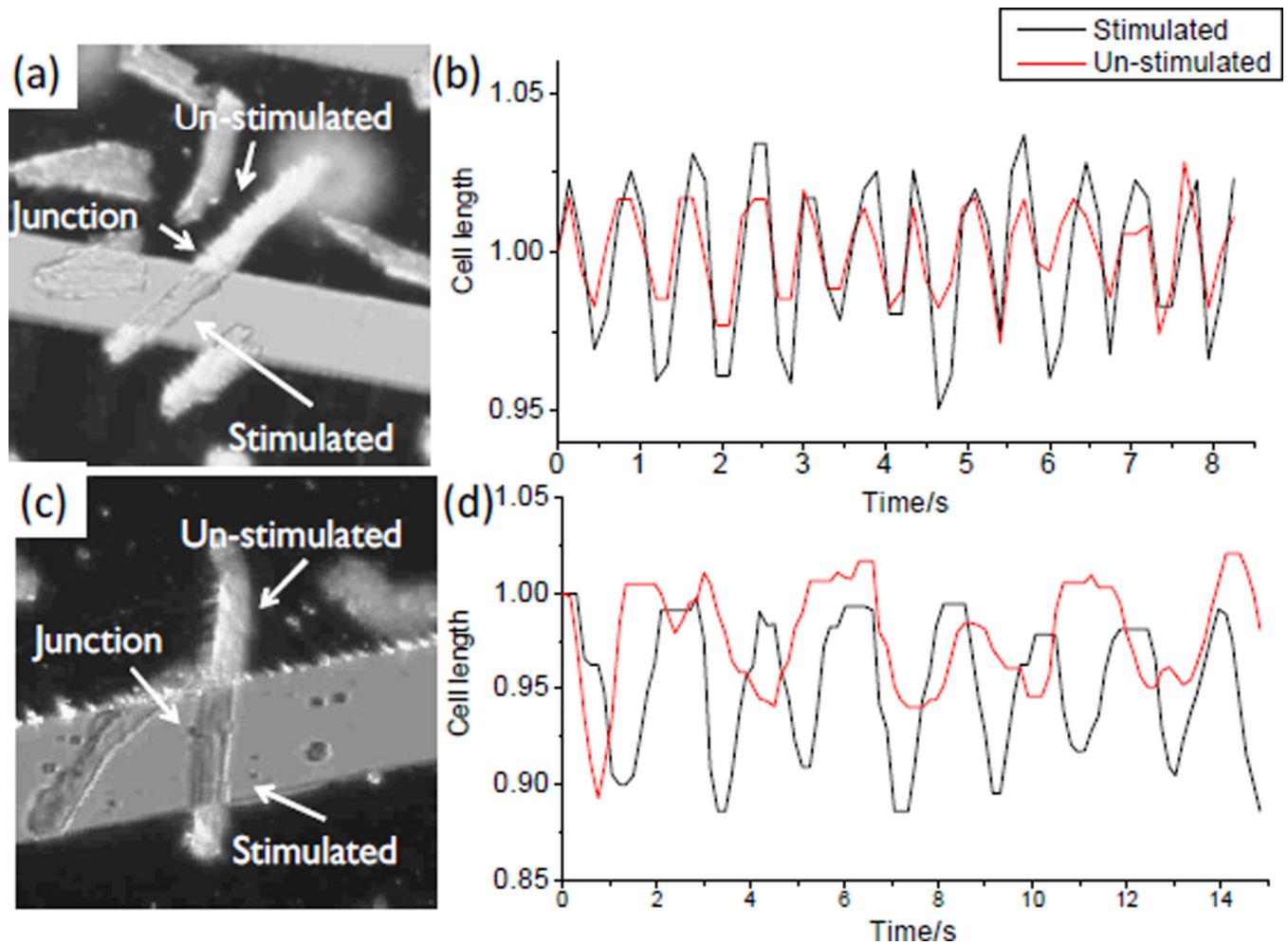
Fig. 8.
Electrical stimulation of the selected cardiac myocytes in longitudinal connected cell doublets (a, c) Micrographs showing cell doublets positioned on top of the microchip with one cell residing between the neighboring electrodes (stimulated) and the other one on top of an electrode finger (un-stimulated); (b) Contractile performance of the two cells recorded in (a) showing a synchronous contraction; and (d) Contractile performance of the two cells recorded in (c) showing an asynchronous contraction.